BOUNDARY POINT DETECTION FOR ULTRASOUND IMAGE SEGMENTATION USING GUMBEL DISTRIBUTIONS

Brian Booth and Xiaobo Li
Department of Computing Science, 2-21 Athabasca Hall, University of Alberta, Edmonton AB, Canada, T6G 2E8

Keywords: Ultrasound Image Processing, Boundary Point Detection, Gumbel Distribution, log-Wiebull Distribution, A-Mode Ultrasound, Data Fitting, Segmentation.

Abstract: Due to high noise, low contrast, and other imaging artifacts, region boundaries in ultrasound images often do not conform to the assumptions of many image processing algorithms. Specifically, the beliefs that region boundaries have a high gradient magnitude or a high intensity can break down in this context.
In this paper, we present an alternative way of detecting likely boundary points in ultrasound images by decomposing the image into one-dimensional intensity scans. These intensity scans, mimicking traditional A-Mode ultrasound, are modeled using Gumbel distributions. Results show that the relationship between the modes of these distributions and regions boundaries is relatively strong.

1 INTRODUCTION

Ultrasound image processing, particularly the task of segmentation, has gained support in both the medical and agricultural fields. In the medical field, computer generated segmentation results are used to help diagnose heart disease as well as breast and prostate cancer (Noble and Boukerroui, 2006). Meanwhile, the agricultural field uses segmentation results to determine the size of various cuts of meat in live animals.

Current image segmentation algorithms applied in this field use assumptions about the appearance of a region or its boundary that are common to general image processing. One popular assumption used here is that a region boundary is characterized by a strong gradient. This is the foundation of many active contour methods (Kass et al., 1987). Also popular is the belief that a region boundary has a high intensity, which has most notably been incorporated into Itti & Koch's saliency map algorithm and has a biological basis (Itti and Koch, 2000). This assumption is of particular interest in ultrasound image segmentation as likely region boundaries tend to appear brighter in ultrasound images than their surroundings (Middleton et al., 2004).

Algorithms based on these two assumptions have been used for ultrasound image segmentation with some success. Gradient-based methods have achieved good results on a limited subset of ultrasound images - particularly echocardiographs - where gradient information is reliable boundary indicator (Yan and Zhuang, 2003; Corsi et al., 2002). Intensity-based algorithms have achieved mild success on both agricultural and medical ultrasound images, but there is room for improvement (Booth et al., 2006).

Unfortunately, these segmentation approaches are limited due to the unique nature of ultrasound images. These images are obtained in a different medium than other real world images and have distinct types of noise and imaging artifacts. Assumptions that have held for the segmentation of other real world images, particularly that regions boundaries have a high gradient magnitude or high intensity, though appropriate for some ultrasound images, generally do not hold. As a result, it is important to return to the question: *What constitutes an edge in an ultrasound image?*

In this paper, we present one approach for detecting edge points in ultrasound images for the purpose of segmentation. In this approach, a given ultrasound image is decomposed into one-dimensional intensity scans with the goal of replicating the original acoustical signals obtained by the ultrasound transducer as

Booth B. and Li X. (2007).
BOUNDARY POINT DETECTION FOR ULTRASOUND IMAGE SEGMENTATION USING GUMBEL DISTRIBUTIONS.
In *Proceedings of the Second International Conference on Signal Processing and Multimedia Applications*, pages 175-179
DOI: 10.5220/0002138701750179

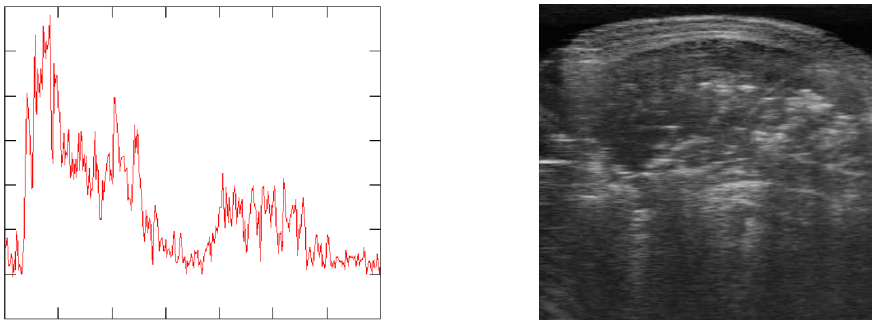

(a) A-Mode Ultrasound (b) B-Mode Ultrasound

Figure 1: Ultrasound Imaging Types.

well as possible. These intensity scans are then modeled as a probability distribution obtained from multiple independent Gumbel distributions, each distribution representing a likely region boundary. Using Expectation-Maximization, a predetermined number of Gumbel density functions are fitted to each intensity scan. The modes of the fitted distributions are then taken as likely boundary points.

The algorithm was implemented and tested on 304 ultrasound images of *in vivo* pork loins and compared with boundary point selection algorithms based solely on intensity or gradient magnitude. Our results suggest that there is a stronger relationship between the modes of the fitted Gumbel distributions and region boundary points than there is with the other two methods.

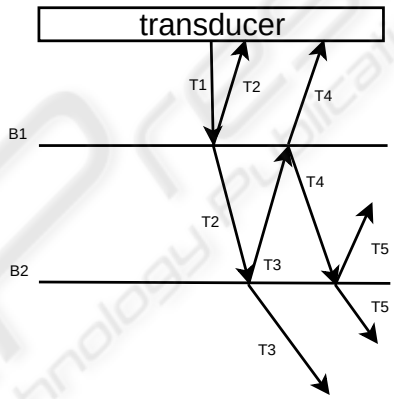

Figure 2: The Reflection and Refraction of Sound Waves from an Ultrasonic Scanner. As in (Muzzolini, 1996).

2 METHOD

To recognize the content of ultrasound images, it becomes important to understand the process through which these images are formed. Therefore, a brief introduction to the physics behind ultrasound imaging is presented here prior to introducing the boundary point detection algorithm.

2.1 Ultrasound Basics

The most common ultrasound imaging technique is known as pulse-echo ultrasound. A simplified example of this ultrasound technique is presented in Figure 2.

A single sound pulse, whose primary direction is shown as T1, leaves the ultrasound transducer and proceeds to enter the subject being scanned. As the sound pulse continues outward, the density of the medium through which the pulse travels will change. This occurs most significantly at boundaries between two tissues of different densities. When the pulse reaches these types of acoustical boundaries, a portion of the pulse reflects back towards the transducer while a now weakened pulse refracts further into the subject. Once the reflected portion of the sound wave, referred to as an echo, returns to the transducer, its amplitude is recorded and using the formula $distance = 2 * velocity * time$, the depth at which the echo was produced can be determined (Muzzolini, 1996).

Using a single transducer, the best we can do is a one-dimensional scan known as an A-Mode (amplitude mode) scan. An example of such a scan is presented in Figure 1(a). To create a two-dimensional image, known as a B-Mode (brightness mode) scan, an array of transducers are used. As a result, an ultrasound image is often considered as an array of A-Mode ultrasound scans. An example of B-Mode ultrasound is shown in Figure 1(b). Pixel intensity in an ultrasound image corresponds directly to the amplitude of the echoes received by the associated transducer. In an ultrasound image, the transducer array can be

pictured as being at the top with each column of the image representing an A-Mode ultrasound scan.

This form of image acquisition is susceptible to noise for many reasons. First, most of our internal tissues do not have a homogeneous density, resulting in echoes being recorded that are not near tissue boundaries. The superposition of echoes that originated from different transducers also adds a particular type of high intensity noise known as *speckle noise*. However, the most problematic issue with ultrasound in terms of noise is movement of the subject. Simply breathing can move tissue boundaries in ways that distort the image (Middleton et al., 2004).

There are also many imaging artifacts common to ultrasound, of which we mention two of particular interest. First, note in Figure 2 that the strength of the echoes recorded by the transducer will depend on the angle at which the sound pulse meets a tissue boundary. As a result, the amplitude of an echo, and in turn the pixel intensity in an ultrasound image, will be lower the less perpendicular a tissue boundary is to the incident sound pulse.

Secondly, as an echo returns to the transducer, it is common for a portion of the echo to reflect off the transducer surface and reverberate between the transducer and the skin of the subject. This results is a decay in amplitude after a strong echo is received instead of a sharp drop-off (Muzzolini, 1996).

These two artifacts, combined with the amount of noise common in ultrasound images, are the key reasons why gradient magnitude and intensity may not, on their own, be able to detect region boundaries. Furthermore, the two imaging artifacts mentioned here produce a distinctive pattern of echo responses for a likely tissue boundary. In particular, the orientation dependence of the echoes results in a gradual rise and fall in echo intensity around the depth of the tissue boundary, while the reverberation of these echoes leads to a decay in echo intensity following the tissue boundary. This phenomenon can be seen in Figure 1(a).

2.2 Algorithm Description

The goal of the algorithm presented herein is to obtain boundary points in ultrasound images by taking advantage of the aforementioned physical properties of ultrasound imaging. To achieve this goal, we decompose the given ultrasound images into its separate columns and treat these columns as A-Mode ultrasound scans. Despite losing some spatial information through this decomposition, we hope to gain an advantage by mimicking the original acoustical signal as much as possible. Henceforth, we will be considering one-dimensional scans similar to the one presented in Figure 1(a).

By visual inspection, we note that the echo pattern for a likely tissue boundary in an A-Mode scan is similar in shape to the Gumbel probability distribution, which is given by the following probability density function:

$$f(x;\mu,\beta) = \frac{e^{-\frac{x-\mu}{\beta}} e^{-e^{-\frac{x-\mu}{\beta}}}}{\beta} \quad (1)$$

The parameters, μ and β, represent the mode and the spread of the density function respectively. A graph of a sample Gumbel probability density function is presented in Figure 3.

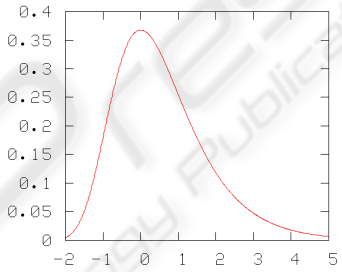

Figure 3: A Sample Gumbel Distribution ($\mu = 0, \beta = 1$).

Due to the similarities in shape, we model the intensity distribution for the echoes from a potential tissue boundary as a Gumbel distribution. An independent collection of Gumbel distributions are fitted to each A-Mode ultrasound scan using Expectation-Maximization. Though it is clear that the echoes created from deeper tissue boundaries are not independent of the echoes from earlier tissue boundaries, the intensity distributions from these echoes still retain the same shape.

To use Expectation-Maximization, the number of Gumbel distributions to fit to - and thereby the number of tissue boundaries in - each A-Mode scan must be known ahead of time. The following algorithm is used to estimate this number:

```
for i = 1:20,
  - Fit a polynomial of degree i
    to the A-Mode scan
  - err[i] = average error between
    the fitted polynomial and the
    A-Mode scan
endfor

minDeg = i, where err[i] == min(err);
numGD = ceil(minDeg / 2);
```

Polynomials of various degrees are fitted to each A-Mode scan using the Least Mean Squared algo-

Table 1: Results for five different boundary point selection algorithms over 304 ultrasound images of in vivo pork loins.

Boundary Point Detection Algorithm	Distance from Actual Boundary (in pixels) Mean	Std. Deviation	Maximum	Percentage Outliers
Gumbel Dist. Fitting	10.661 ± 2.329	7.356 ± 1.916	34.668 ± 8.661	87.768 ± 2.185
Intensity (equal number)	29.268 ± 8.844	27.823 ± 7.792	98.226 ± 23.406	87.270 ± 2.262
Gradient (equal number)	16.168 ± 5.964	15.374 ± 6.699	62.001 ± 23.034	88.837 ± 2.205
Intensity (top 13%)	3.922 ± 2.002	6.210 ± 3.235	28.209 ± 12.441	97.172 ± 0.252
Gradient (top 13%)	1.795 ± 0.581	2.155 ± 0.945	11.904 ± 4.891	97.350 ± 0.224

rithm. While these polynomials do not relate well to the tissue boundaries represented in the scan, the degree of the polynomial of best fit can be related to the number of Gumbel distributions to fit to the scan. The polynomial's degree is divided by two on account of the Gumbel distribution's roughly parabolic shape. An example of an A-Mode scan fitted with Gumbel distributions is shown in Figure 4.

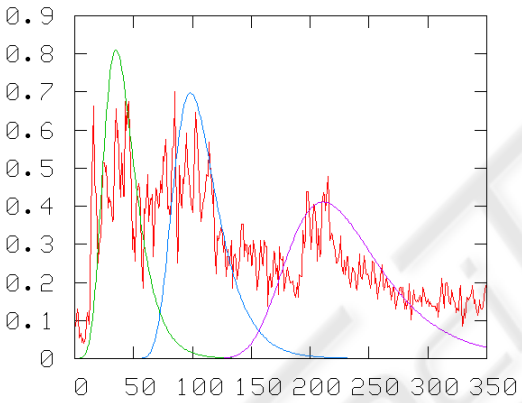

Figure 4: An A-Mode Scan Fitted with Three Gumbel Distributions. The Gumbel Distributions are Scaled for Viewing Purposes.

The modes of the fitted Gumbel distributions are taken as the most likely locations of the tissue boundaries the distributions represent.

3 EXPERIMENTAL RESULTS

The proposed boundary point detection algorithm was implemented and tested on a set of 304 ultrasound images of *in vivo* pork loins. The ultrasound images were recorded with an Aloka Flexus Model SSD-1100 equipped with a 3.5MHz/127mm transducer Ultrasound system. The images are from between the 3rd and 4th ribs from the last rib and 7cm off the midline of the pigs. This collection of images includes the thirty-eight images used in (Booth et al., 2006).

For each image, we compare the detected boundary points with a manually traced contour created by an expert. The distance between each point on the manually traced contour and the closest boundary point is measured. The average, standard deviation, and maximum values of these distances are calculated for each image. Also calculated is the percentage of detected boundary points that are not the closest boundary point for any of the points on the manually traced contour.

The set of boundary points obtained by the proposed algorithm are compared with those obtained by thresholding based on intensity and gradient magnitude. Two thresholds are used: one which provides an equal number of boundary points, and one that gives thirteen percent of the image's pixels as boundary points. The second threshold is essentially the same one used on intensity in (Booth et al., 2006).

Table 1 displays results for all five approaches. Means and standard deviations for each measure are provided over all images in the set.

Given an equal number of detected boundary points, the intensity and gradient methods detect points that have a much larger average distance to the contour as well as a larger standard deviation than the proposed approach, suggesting in those two cases that large portions of the contour do not have any detected boundary points nearby. Increasing the number of likely boundary points in the intensity and gradient methods does seem to alleviate this problem, but also introduces a significant amount of outliers, which suggests that the relationship between those measures and the contour are not as strong as with the proposed algorithm.

Visual inspection appears to confirm that this is in fact what is happening. Figure 5 shows the results from all five algorithms on an average case. Despite obvious outliers due to noise and other anatomical structures, boundary points are detected near large portions of the contour using the presented approach.

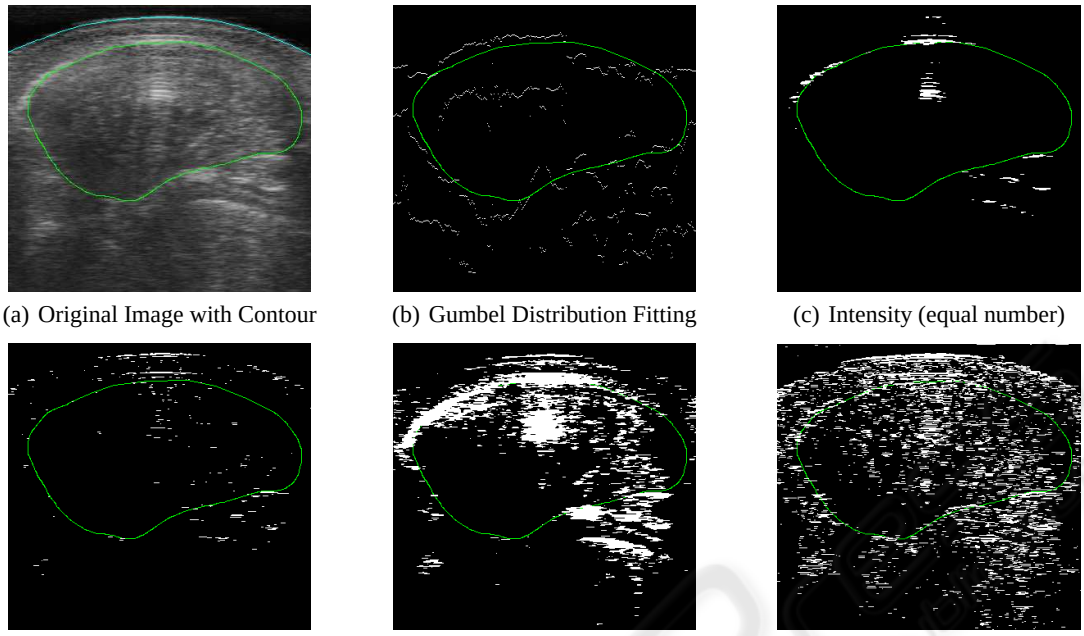

(a) Original Image with Contour (b) Gumbel Distribution Fitting (c) Intensity (equal number)

(d) Gradient (equal number) (e) Intensity (13%) (f) Gradient (13%)

Figure 5: Sample Boundary Point Detection Results from an Average Case for our Algorithm and Four Others. The Contour is Displayed in Green while the Detected Boundary Points are Shown in White.

4 CONCLUSION

Given the different medium from which ultrasound images are created, general assumptions about how an edge is represented break down. Using knowledge of how the images are acquired, we present a boundary point detection algorithm that fits Gumbel distributions to mimicked A-Mode scans obtained from an ultrasound image. Results on 304 *in vivo* pork loin ultrasound images show that the relationship between the modes of the Gumbel distributions and actual boundary points is stronger than methods based on other general image processing assumptions.

ACKNOWLEDGEMENTS

We gratefully acknowledge Dr. Alan Tong of Lacombe Research Centre, Agriculture and Agri-Food Canada for providing the ultrasound image data for this study. Also, thanks to the Natural Sciences and Engineering Research Council of Canada (NSERC) and the Informatics Circle of Research Excellence (iCORE) for funding this project.

REFERENCES

Booth, B., Neighbour, R., and Li, X. (2006). On agricultural ultrasound image segmentation. In *Proceedings of IEEE International Conference on Signal Processing*, pages 915–920.

Corsi, C., Saracino, G., Sarti, A., and Lamberti, C. (2002). Left ventricular volume estimation for real-time three-dimensional echocardiography. *IEEE Transactions on Medical Imaging*, 21(9):1202–1208.

Itti, L. and Koch, C. (2000). A saliency-based search mechanism for overt and covert shifts of visual attention. *Vision Research*, 40:1489–1506.

Kass, M., Witkin, A., and Terzopoulos, D. (1987). Snakes: Active contour models. In *Proceedings of the IEEE International Conference on Computer Vision*, pages 259–268.

Middleton, W. D., Kurtz, A. B., and Hertzberg, B. S. (2004). *Ultrasound, The Requisites*, chapter Practical Physics, pages 3–26. Mosby, Inc., 2 edition.

Muzzolini, R. E. (1996). *A Volumetric Approach to Segmentation and Texture Characterisation of Ultrasound Images*. PhD thesis, University of Saskatchewan.

Noble, J. A. and Boukerroui, D. (2006). Ultrasound image segmentation: A survey. *IEEE Transactions on Medical Imaging*, 25(8):987–1010.

Yan, J. Y. and Zhuang, T. (2003). Applying improved fast marching method to endocardial boundary detection in echocardiographic images. *Pattern Recognition Letters*, 24(15):2777–2784.